

## A Superprotein Triangle Driven by Nickel(II) Coordination: Exploiting Non-Natural Metal Ligands in Protein Self-Assembly

Robert J. Radford and F. Akif Tezcan\*

Department of Chemistry and Biochemistry, University of California, San Diego, 9500 Gilman Drive, La Jolla, California 92093-0356

Received January 5, 2009; E-mail: tezcan@ucsd.edu

Nature utilizes proteins as building blocks to construct a wide variety of self-assembled nanoscale architectures. Despite advances in protein design and engineering,<sup>1</sup> attaining the structural and functional sophistication of such multiprotein architectures remains a distant goal. To bypass the immense challenge of controlling the noncovalent interactions that hold these assemblies together, we have devised a strategy, which we now call “metal-directed protein self-assembly” (MDPSA), that utilizes the simultaneous stability, lability, and directionality of metal–ligand bonds to drive protein–protein interactions.<sup>2</sup> The use of metal coordination to control protein self-assembly is attractive from both structural and functional perspectives: whereas the directionality and symmetry inherent in metal coordination can govern the overall supramolecular geometry, the resulting interfacial metal centers may potentially offer new reactivities within biological scaffolds. With these advantages in mind, we asked whether the structural and functional scope of MDPSA can be further augmented with non-natural metal ligands. Here we report the Ni-dependent self-assembly properties of a cytochrome *cb*<sub>562</sub> variant, MBP-Phen1, which features a covalently attached phenanthroline (Phen) group on its surface. MBP-Phen1 not only forms an unusual supramolecular architecture as a result of specific Phen–protein interactions but also presents coordinatively unsaturated Ni centers within this assembly.

To site-selectively nucleate metal binding on protein surfaces, we previously adopted the strategy of employing multidentate motifs (e.g., an *i, i + 4* di-His arrangement on a helix) to outcompete the mostly monodentate side-chain functionalities for metal coordination.<sup>2</sup> We then imagined that non-natural multidentate motifs such as Phen that have a single-point attachment would offer more structural flexibility than a di-His motif while also allowing nonproteinaceous functionalities to be incorporated into protein assemblies.<sup>3</sup> A cysteine-specific iodoacetamide derivative of Phen (IA-Phen) was previously used to generate stable metal binding sites on proteins.<sup>4</sup> Using IA-Phen, we constructed MBP-Phen1, which contains a single Phen group covalently bound to Cys59 (PhenC59) near the N-terminus of Helix3 as well as His77 incorporated at the opposite end to induce head-to-tail arrangements [Figure S1a in the Supporting Information (SI)]. Additionally, MBP-Phen1 contains a His at position 66 (two helix turns away from Cys59) with the idea that this residue could potentially form an *i, i + 7* tridentate acceptor motif together with PhenC59.

Titrations with late first-row transition metals indicated that Ni(II) in particular tightly associates with MBP-Phen1 and leads to significant enhancement in overall protein stability, likely through *i, i + 7* His66–PhenC59 cross-linking (Figures S2 and S3). The multitude of possible Ni-mediated protein oligomerization modes (Figure S1b) and the non-negligible interactions that could be formed between protein surfaces in these states make the a priori assignment of the thermodynamically preferred superstructure

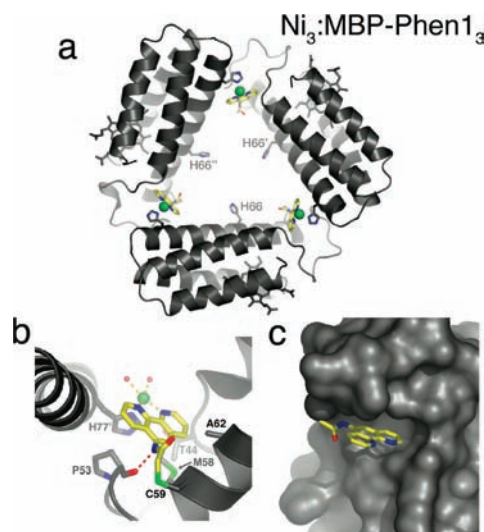


**Figure 1.** (a) Top view of Ni<sub>3</sub>:MBP-Phen1<sub>3</sub>. Ni ions are shown as green spheres, and PhenC59 is highlighted in yellow. (b) Coordination environment of Ni–PhenC59. The H bond between the P53 carbonyl and the PhenC59 amide nitrogen is indicated with a red dashed line. Aquo and chloride ligands are shown as red spheres. (c) Burial of PhenC59 under the 50s loop.

challenging. Therefore, we sought to determine the crystal structure of the Ni adduct of MBP-Phen1.

Crystals of MBP-Phen1 were obtained in two space groups (*P*<sub>2</sub><sub>1</sub> and *P*<sub>6</sub><sub>3</sub><sub>2</sub>) from two similar but different solutions containing equimolar protein and Ni, and their structures were determined at 2.4 and 3.15 Å resolution, respectively. Both structures (PDB entries 3FOO and 3FOP) reveal a unique triangular assembly, Ni<sub>3</sub>:MBP-Phen1<sub>3</sub>, having perfect C<sub>3</sub> symmetry (Figure 1). Each vertex of this triangle is formed through coordination of a Ni atom to PhenC59 from one protein monomer and His77 (Nδ) from another (Figure 1b), whereby the three Ni atoms lie on the plane of the triangle ~30 Å from one another. Ni–protein coordination appears to be the primary driving force for self-assembly, as the docking interactions between the protein monomers are minimal and nonspecific.

The Phen group, instead of extending into the solvent, is positioned in a small hydrophobic crevice underneath the 50s loop and further stabilized by a H bond between the PhenC59 amide nitrogen and the Pro53 backbone carbonyl (Figure 1b,c). In accord with these favorable interactions, MBP-Phen1 was found through unfolding titrations to be ~1.5 kcal/mol more stable than its unlabeled counterpart (Figure S2). The placement of Phen is the key to the open Ni<sub>3</sub>:MBP-Phen1<sub>3</sub> architecture: it protects the Ni ion from coordination by a second Phen group (or His66) and allows only one other protein monomer to coordinate through His77 in the cis position, which ultimately results in an unsaturated, roughly

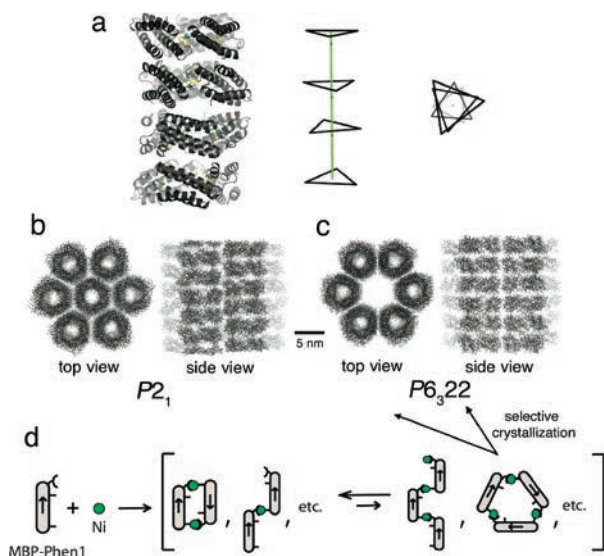


**Figure 2.** (a) Four  $\text{Ni}_3\text{:MBP-Phen1}_3$  trimers in the asymmetric unit of the  $P2_1$  crystals and their triangular representation (Ni atoms as vertices) viewed from the side and the top. (b, c) Lattice packing arrangements of  $\text{Ni}_3\text{:MBP-Phen1}_3$  in the  $P2_1$  and  $P6_322$  crystal forms. (d) Suggested Ni-induced oligomerization behavior of MBP-Phen1 in solution.

square-pyramidal Ni coordination geometry. While His77 ( $d_{\text{Ni-N}} = 2.1 \pm 0.1 \text{ \AA}$ ) and PhenC59 ( $d_{\text{Ni-N1/N2}} = 2.1 \pm 0.1 \text{ \AA}$ ) are clearly defined in the electron density maps (Figure S11), the two other coordination sites cannot be unambiguously assigned because of the resolution limits. We tentatively ascribe the diffuse electron density near Ni to two aquo/chloride ligands coordinated trans to PhenC59 at distances of 2.8 and 2.6 ( $\pm 0.3$ )  $\text{\AA}$  from Ni and 2.7 ( $\pm 0.2$ )  $\text{\AA}$  from each other, averaged over the 12 independent metal sites in the asymmetric unit of  $P2_1$  crystals (see the SI for a detailed discussion).

Lattice packing interactions in both  $\text{Ni}_3\text{:MBP-Phen1}_3$  crystals are particularly noteworthy. In the  $P2_1$  form, there are four crystallographically distinct but identical (overall rmsd- $C_\alpha = 0.3 \text{ \AA}$ ) copies of the trimer in the asymmetric unit, which stack up along their threefold symmetry axes to form a tubular architecture (Figure 2a). Each of the four  $\text{Ni}_3\text{:MBP-Phen1}_3$  trimers adopts a different orientation around the long axis of the tube, giving rise to three distinct trimer–trimer interactions. In the lattice, the tubular units are further stacked end-on-end infinitely and, because of the superposition of the four different trimer orientations, adopt an apparent hexagonal geometry. The resulting hexagonal tubes form a tightly packed two-dimensional array (50% solvent content) (Figure 2b). In the  $P6_322$  crystals, the  $\text{Ni}_3\text{:MBP-Phen1}_3$  trimers are similarly arranged to form hexagonal tubular structures (Figure 2c). In contrast to the  $P2_1$  lattice, the trimers of all adjacent tubes are coplanar, which is required for generation of the two-, three- and sixfold symmetry components of the  $P6_322$  space group. Moreover, a central hexagonal tube is not accommodated in this lattice, leading to a large cavity (6 nm diameter) and an increased crystal solvent content of 64%. Though observed only in crystals, such arrangements suggest that open, symmetrical protein superstructures such as  $\text{Ni}_3\text{:MBP-Phen1}_3$  could be in principle be utilized as building blocks for porous protein frameworks.

The fact that the same  $\text{Ni}_3\text{:MBP-Phen1}_3$  structure is found in several different lattice packing environments in two crystal forms provides strong evidence for both its existence in solution and its

rigidity. Sedimentation velocity measurements, on the other hand, indicate that the predominant species at low protein/Ni concentrations ( $< 1 \text{ mM}$ ) is dimeric (Figure S10). We suggest that the trimeric forms (including  $\text{Ni}_3\text{:MBP-Phen1}_3$ ), which should be entropically disfavored relative to any dimeric species, are only significantly populated at the high protein concentrations required for crystallization.<sup>5</sup> The high internal symmetry of  $\text{Ni}_3\text{:MBP-Phen1}_3$  and its rigidity likely promote its selective crystallization from among other species that coexist in solution (Figure 2d). Studies are currently underway to stabilize  $\text{Ni}_3\text{:MBP-Phen1}_3$  and destabilize other possible conformations through surface engineering in order to isolate it in solution and assess the reactivity of the interfacial Ni centers.<sup>6</sup>

Synthetic metal-coordinating functionalities have previously been employed to stabilize coiled-coil assemblies,<sup>7</sup> construct reactive metal binding sites in protein interiors,<sup>4a</sup> and tune the potentials of redox centers,<sup>8</sup> among other applications.<sup>3</sup> We have demonstrated here that incorporation of such non-natural ligands onto protein surfaces can lead to novel biological architectures as well as coordinatively unsaturated metal sites within these scaffolds. The wide array of functionalities available in the synthetic inorganic chemist's toolbox thus could provide a powerful means of generating structural and functional diversity in protein self-assembly.

**Acknowledgment.** This work was supported by UCSD, a Beckman Young Investigator Award (F.A.T.), and an NIH Heme and Blood Program Training Grant (R.J.R.). Portions of this research were carried out at SSRL, operated by Stanford University on behalf of DOE.

**Supporting Information Available:** Additional experimental details and discussion. This material is available free of charge via the Internet at <http://pubs.acs.org>.

## References

- (a) Ghirlanda, G.; Lear, J. D.; Ogihara, N. L.; Eisenberg, D.; DeGrado, W. F. *J. Mol. Biol.* **2002**, *319*, 243. (b) Andre, I.; Bradley, P.; Wang, C.; Baker, D. *Proc. Natl. Acad. Sci. U.S.A.* **2007**, *104*, 17656.
- (a) Salgado, E. N.; Faraone-Mennella, J.; Tezcan, F. A. *J. Am. Chem. Soc.* **2007**, *129*, 13374. (b) Salgado, E. N.; Lewis, R. A.; Faraone-Mennella, J.; Tezcan, F. A. *J. Am. Chem. Soc.* **2008**, *130*, 6082.
- Lu, Y. *Curr. Opin. Chem. Biol.* **2005**, *9*, 118.
- (a) Qi, D. F.; Tann, C. M.; Haring, D.; DiStefano, M. D. *Chem. Rev.* **2001**, *101*, 3081. (b) Chen, C. H. B.; Milne, L.; Landgraf, R.; Perrin, D. M.; Sigman, D. S. *ChemBioChem* **2001**, *2*, 735.
- Since the dimeric and trimeric species are in equilibrium, as dictated by the exchange lability of Ni(II), we carried out kinetic trapping experiments to isolate any metal-induced oligomeric forms. To this end, we alternately utilized (a) homobifunctional imidoester crosslinkers (DMS, DMP, DMA) aimed at linking Lys pairs across protein interfaces and (b) Ru(II) as a substitution-inert surrogate for Ni(II) (see the SI). In accord with the scenario in Figure 2d, electrophoresis results indicated that all three crosslinkers and Ru(II) led to the capture of predominantly dimeric and some trimeric products. In the case of the covalent crosslinkers, Ni(II) was required for trapping both dimeric and trimeric species. We subsequently isolated the trimeric species from Ru- as well as DMS-treated MBP-Phen1 samples by chromatography and subjected them to metal analysis and hydrodynamic measurements. ICP-OES measurements on thoroughly dialyzed samples yielded Ni/protein and Ru/protein ratios of 1.1 and 1.4 for the DMS- and Ru-cross-linked species, respectively. Sedimentation coefficient distributions for both species were centered at 3.3 S, in good agreement with hydrodynamic calculations based on the  $\text{Ni}_3\text{:MBP-Phen1}_3$  crystal structure. While these studies by themselves do not prove that the cross-linked trimeric species include  $\text{Ni}_3\text{:MBP-Phen1}_3$ , they are consistent with its composition and shape.
- Preliminary IR studies (Figure S13) using  $\text{Ni}_3\text{:MBP-Phen1}_3$  crystals suggest that the Ni sites can coordinate isocyanate ligands within the crystal lattice.
- (a) Ghadiri, M. R.; Soares, C.; Choi, C. *J. Am. Chem. Soc.* **1992**, *114*, 4000. (b) Lieberman, M.; Sasaki, T. *J. Am. Chem. Soc.* **1991**, *113*, 1470. (c) Mutz, M. W.; McLendon, G. L.; Wishart, J. F.; Gaillard, E. R.; Corin, A. F. *Proc. Natl. Acad. Sci. U. S. A.* **1996**, *93*, 9521.
- Privett, H. K.; Reedy, C. J.; Kennedy, M. L.; Gibney, B. R. *J. Am. Chem. Soc.* **2002**, *124*, 6828.

JA9000695